



Cr³⁺ CENTERS IN THE LaMgAl₁₁O₁₉ LASER HOST : THEORETICAL STUDY THROUGH A MOLECULAR ORBITAL MODEL

F. Michel-Calendini, K. Bellafruh, V. Poncon, G. Boulon

► To cite this version:

F. Michel-Calendini, K. Bellafruh, V. Poncon, G. Boulon. Cr³⁺ CENTERS IN THE LaMgAl₁₁O₁₉ LASER HOST : THEORETICAL STUDY THROUGH A MOLECULAR ORBITAL MODEL. Journal de Physique Colloques, 1987, 48 (C7), pp.C7-497-C7-499. 10.1051/jphyscol:19877118 . jpa-00226935

HAL Id: jpa-00226935

<https://hal.science/jpa-00226935>

Submitted on 4 Feb 2008

HAL is a multi-disciplinary open access archive for the deposit and dissemination of scientific research documents, whether they are published or not. The documents may come from teaching and research institutions in France or abroad, or from public or private research centers.

L'archive ouverte pluridisciplinaire **HAL**, est destinée au dépôt et à la diffusion de documents scientifiques de niveau recherche, publiés ou non, émanant des établissements d'enseignement et de recherche français ou étrangers, des laboratoires publics ou privés.

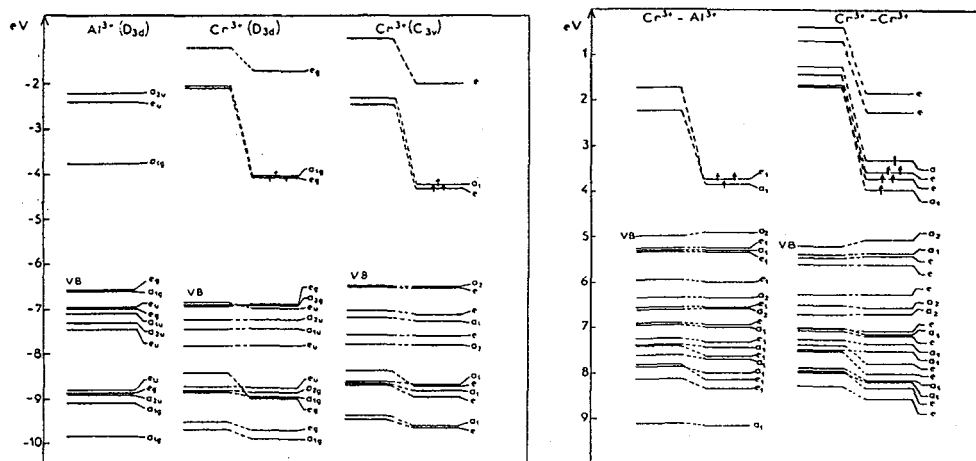
Cr³⁺ CENTERS IN THE LaMgAl₁₁O₁₉ LASER HOST : THEORETICAL STUDY THROUGH A MOLECULAR ORBITAL MODEL

F. MICHEL-CALENDINI, K. BELLAFFROUH, V. PONÇON and G. BOULON

*Laboratoire de Physico-Chimie des Matériaux Luminescents,
CNRS UA-442 et Greco Celphyra, Université Claude Bernard,
Lyon I, F-69622 Villeurbanne Cedex, France*

The fluorescence and absorption spectra of LaMgAl₁₁O₁₉ crystal doped with Cr³⁺ and EPR investigations gives evidence for the presence of Cr³⁺ multisites ¹⁾: Cr ions are trapped at the 2a, 4f and 12k Al octaedral sites and Cr-Cr pair centers at 4f sites are also assumed. The electronic structures of these different centers are determined through a molecular orbital model using the spin polarized option of the SCF X α method. The computational framework is similar to the one described for Cr³⁺ in perovskite oxydes ²⁾. The only difference consist in the choice of a local spin density approximation ³⁾ which improves agreement between experimental and calculated term splittings for states with large spin polarizations as Cr³⁺.

Eigenvalue diagrams are obtained for the ⁴A₂ ground term as shown in figures 1 and 2. AlO₆⁹⁻ (D_{3d}) and CrO₆⁹⁻ (D_{3d}) represent the undoped and doped 2a site while CrO₆⁹⁻ (C_{3v}) is associated to the 4f site. AlCrO₉¹²⁻ and Cr₂O₉¹²⁻ picture two adjacent 4f sites doped with one or two Cr³⁺ ions respectively. Atomic distances used in the cluster geometries are taken from Khan et al ⁴⁾. These diagrams show the d $\epsilon\uparrow$ (d $\epsilon\downarrow$) splittings into a₁ and e levels increase slightly from 2a to 4f sites while the two groups of d ϵ levels associated to Cr-Cr pair are spreaded on more than 0.2 eV ; an important covalency of Cr-Cr and Cr-O bonds is noticed in the latter. The energies of excited terms relatively to ⁴A₂ have been evaluated from suitable transition state computations between d $\epsilon\uparrow^3$, d $\epsilon\uparrow^2$ d $\epsilon\downarrow$ and d $\epsilon\uparrow^2$ d $\epsilon\uparrow$ configurations. It is possible to deduce the B and C Racah parameters and the Dq crystal field strength from the transitions associated to the 2a site. Assuming C/B = 4.5, we obtain B = 774cm⁻¹ and 10 Dq = 15910cm⁻¹. The electrostatic interactions provide the term energy diagram of figure 3a. On the other hand, the fluorescence emission line at 689nm, associated to ²E \rightarrow ⁴A₂ emission (2a site) and the absorption peak at 565nm, attributed to ⁴A₂ \rightarrow ⁴T₂ are used to obtain B_{exp} = 695nm, 10 Dq = 17700cm⁻¹ and the relevant term energy diagram of figure 3b. Both theoretical and experimental term positions are compared to the absorption spectrum in this figure and allow the assignments of all the experimental structures. Nevertheless, it may be noticed



Figures 1 and 2 : $02p$, $Cr3d$ and $Al3s$, $Al3p$ eigenvalues in various cluster representative of undoped and doped $2a$, $4f$ and coupled $4f$ sites in $LaMgAl_{11}O_{19}$.

that the ${}^4A_2 \rightarrow {}^4T_2$ energy is overestimated since the peak maximum lies at shorter wavelength than the zero-phonon line, unresolved in the spectrum, but expected around 650nm ⁵⁾; this would imply $Dq \sim 1540\text{ cm}^{-1}$, much more in agreement with the theoretical data.

For the $4f$ site, the ${}^2E \rightarrow {}^4A_2$ emission line is calculated to be 0.075eV lower than in the $2a$ case. This follows the experimental trends where the wavelength of this line varies from 689 to 695 nm compared to the 623 to 647 nm calculations in the $2a$ and $4f$ sites respectively. Simultaneously, ${}^4A_2 \rightarrow {}^4T_2$ would be spreaded by the splitting of 4T_2 into 4A_1 and 4E terms (estimated around 0.08 eV) and a decrease of its mean energy is predicted. This correlates the experimental observations.

The overall splitting of $d\epsilon\uparrow$, $d\epsilon\downarrow$ and $d\gamma\uparrow$ levels in the pair center creates broad ${}^2E \rightarrow {}^4A_2$ and ${}^4A_2 \rightarrow {}^4T_2$ bands, which overlap each other. The minimum energy of ${}^4A_2 \rightarrow {}^4T_2$ transitions decreases again relatively to the cubic and pseudocubic cases.

The evolution of the calculated 2E and 4T_2 energies show that $2a$, $4f$ and pair centers behave as more and more low-field chromium complexes in the region $Dq/B \sim 2$ in the Tanabe and Sugano d^3 diagram.

REFERENCES

1. B. Viana, A.M. Lejus, D. Vivien, V. Ponçon and G. Boulon
J. of Sol. State Chem. 60 (1987).

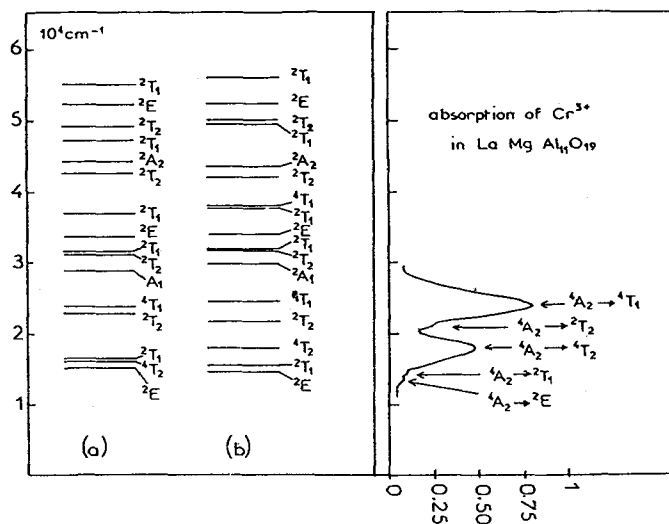


Figure 3 - Theoretical and experimental term diagrams of Cr^{3+} in octahedral symmetry compared to absorption spectrum of $\text{LaMgAl}_{11}\text{O}_{19}:\text{Cr}^{3+}$.

2. P. Moretti and F.M. Michel-Calendini, Phys. Rev. B34, 8538 (1986).
3. S.H. Vosko, L. Wilk and M. Nusair, Can. J. Phys. 58, L1200 (1980).
4. A. Khan, A.M. Lejus, M. Madsae, J. Thery, D. Vivien and J.C. Bernier, J. Appl. Phys. 52, 6864 (1984).
5. G. Boulon in Disordered solids : structures and processes, Ed di Bartolo, Plenum Press - New-York (1988).